COVID-19: Effects of weather conditions on the propagation of respiratory droplets

Lei Zhao[1], Yuhang Qi[1], Paolo Luzzatto-Fegiz[1], Yi Cui[2,3], Yangying Zhu[1*]

[1]Department of Mechanical Engineering, University of California Santa Barbara, Santa Barbara CA 93106, USA

[2]Department of Materials Science and Engineering, Stanford University, Stanford, CA 94305, USA

[3]Stanford Institute for Materials and Energy Sciences, SLAC National Accelerator Laboratory, Menlo Park, CA 94025, USA

*To whom correspondence should be addressed：

Yangying Zhu, Email: yangying@ucsb.edu

KEYWORDS: COVID-19, transmission, respiratory droplets, aerosol, weather

ABSTRACT: As the number of confirmed cases of Coronavirus disease 2019 (COVID-19) continues to increase, there has been a rising concern regarding the effect of weather conditions, especially over the upcoming summer, on the transmission of this disease. In this study, we assess the transmission of COVID-19 under different weather conditions by investigating the propagation of infectious respiratory droplets. A comprehensive mathematical model is established to explore their evaporation, heat transfer and kinematics under different temperature, humidity and ventilation conditions. The transmitting pathway of COVID-19 through respiratory droplets is divided into short-range droplet contacts and long-range aerosol exposure. We show that the effect of weather conditions is not monotonic: low temperature and high humidity facilitate droplet contact transmission, while high temperature and low humidity promote the formation of aerosol particles and accumulation of particles with a diameter of 2.5 μm or less (PM2.5). Our model suggests that the 6 ft of social distance recommended by the Center for Disease Control and Prevention (CDC) may be insufficient in certain environmental conditions, as the droplet spreading distance can be as long as 6 m (19.7 ft) in cold and humid weather. The results of this study suggest that the current pandemic may not ebb in the summer of the northern hemisphere without proper intervention, as there is an increasing chance of aerosol transmission. We also emphasize that the meticulous design of building ventilation systems is critical in containing both the droplet contact infections and aerosol exposures.

Coronavirus disease 2019 (COVID-19) is an ongoing global pandemic with more than 5 million confirmed cases and over 0.3 million deaths as of May 23th,(*1*) within six months since the first case was identified. The disease is caused by the severe acute respiratory syndrome coronavirus 2 (SARS-CoV-2).(*2–5*) One major challenge for the effective containment and mitigation of the virus before vaccines are available is its high transmissibility.(*6–9*) The basic reproduction number R_0, which measures the average secondary infections caused by one infectious case, for COVID-19 has a mean value of 3.28 and may rise to as high as 6.32 without proper public health interventions,(*10–12*) a sobering value compared to R_0 = 1.4-1.7 for influenza and R_0 = 1-3 for the severe acute respiratory syndrome (SARS).(*13*, *14*) Therefore, a detailed and quantitative understanding of the transmission mechanisms of SARS-CoV-2 under realistic circumstances is of paramount importance, particularly as many countries start to ease their mobility restrictions.

Among known transmitting pathways of SARS-CoV-2, transmission via respiratory droplets is believed to be a primary mode, based on previous studies on SARS(*15*) and influenza(*16*). As many as 40,000 respiratory droplets can be generated by sneezing, coughing and even normal talking, with initial speeds ranging from a few meters per second up to more than a hundred meters per second.(*17–19*) These respiratory droplets are expelled from our upper respiratory tracts (URTs) and serve as potential pathogen carriers.(*20*) Extensive studies have been conducted to investigate the formation,(*21, 22*) spreading,(*18–20, 23*) and infectivity (*24, 25*) of respiratory droplets. Models to predict the infection probability under different circumstances have been developed as well.(*26–28*) These past studies suggest that both aerodynamics and the heat and mass exchange process with the environment can determine the mode and the effectiveness of virus propagation during the travel of respiratory droplets. While large droplets usually settle onto a surface within a limited distance due to gravity, smaller droplets evaporate rapidly to form aerosol particles that are able to carry the virus and float in air for hours.(*28, 29*) Under certain weather conditions, how far can the virus carriers travel on average? What fraction of droplets will turn into aerosol particles? What role do the HVAC and air conditioning systems play in virus propagation? Quantitative answers to these practical questions can provide urgently needed guidance to both policy makers and the general public, e.g. on social distancing rules.

In fact, there have already been intensive ongoing debates about the potential impact of weather conditions on the COVID-19 pandemic. Environmental parameters, such as temperature and humidity, can profoundly affect the survival and transmission of the virus, as well as the immune function and social behaviors of the hosts.(*20–23*) As a result, the spreading of SARS and influenza have shown strong dependence on seasonality: SARS vanished in the summer of 2003 and the massive infection of influenza mostly happens in wintertime. However, whether COVID-19 also shows a similar seasonal pattern is still unclear. From the perspective of virus activities, Chin et al.(*30*) reported that the virus is sensitive to heat, but generally SARS-CoV-2 can withstand 37 ℃ of incubation temperature for longer than 1 day. van Doremalen et al reported that the half-life of aerosolized SARS-CoV-2 at 65% relative humidity and 21-23°C is approximately 1.1 to 1.2 hours.(*31*) However, another experimental study by Fears et al (*32*) compared the stability of SARS-CoV-2 with SARS-CoV and MERS-CoV in aerosol and found that SARS-CoV-2 remains infectious even after 16 hours. To this end, the impact of different weather conditions on the infectivity of SARS-CoV-2 is still inconclusive. One study calculated the daily effective

reproductive number R_0 for 100 Chinese cities and argued that high temperature and high humidity reduced the transmission of COVID-19.(*33*) In contrast, another research by Kissler et al (*34*) assumed similar seasonality of COVID-19 with human coronavirus OC43 (HCoV-OC43) and HCoV-HKU1. They highlighted potentially recurrent seasonal outbreaks of COVID-19 until 2024 in spite of the immunity gained from vaccination. It is clear that a comprehensive study on the interactions between weather conditions and the propagation of SARS-CoV-2-containing respiratory droplets can help resolve some of the controversies.

This study investigates the influence of weather conditions including temperature, humidity and wind velocity, on the transmission of SARS-CoV-2-containing respiratory droplets. We integrate aerodynamics, evaporation, heat transfer and kinematic theories into a mathematical model to predict the spreading capabilities of COVID-19 in different weather conditions. We expanded the modeling framework developed by Wells,(*29*) Kukkonen et al(*35*) and Xie et al(*23*) by discussing Brownian motion, considering residual salt and incorporating kinematic analysis of aerosol particles. As shown in Figure 1, the transmission of COVID-19 through respiratory droplets is categorized into two modes: droplet contact and exposure to aerosol particles. We first focus on the effect of temperature and relative humidity on these two modes of disease transmission. Our results suggest that high temperature and low humidity promote the formation of aerosol particles, while low temperature and high humidity promote droplet contact transmission. Although social distancing has been proven effective in slowing down COVID-19 transmission, the 6 feet of physical distance recommended by the Centers for Disease Control and Prevention (CDC) turns out to be insufficient in eliminating all possible droplet contacts. In some extremely cool and humid weather conditions, the droplet spreading distance may reach as far as 6 m (19.7 feet). We suggest that the current pandemic may not ebb over the summer without continuous and proper public health intervention, because (1) in hot and dry weather, respiratory droplets more easily evaporate into aerosol particles capable of long-range transmission; (2) infectious PM2.5 that can infiltrate deeply into our lung has a longer suspension time in hot and dry weather; (3) many public spaces implement air-conditioning systems that can still operate at temperature and humidity setpoints that favor droplet transport. Our results also demonstrate that ventilation has both favorable and adverse consequences. On one hand, ventilation to outdoor air can effectively dilute the accumulation of infectious aerosol particles; on the other hand, improper design of ventilation systems may void the effort of social distancing by expanding the traveling

distance of pathogen-carrying droplets and aerosols. Last but not least, we emphasize that the effect of weather on COVID-19 transmission is not monotonic. To curb the spread of this disease and avoid possible resurgent waves of infections, we advise that flexible public health measures should be taken depending on detailed environmental conditions.

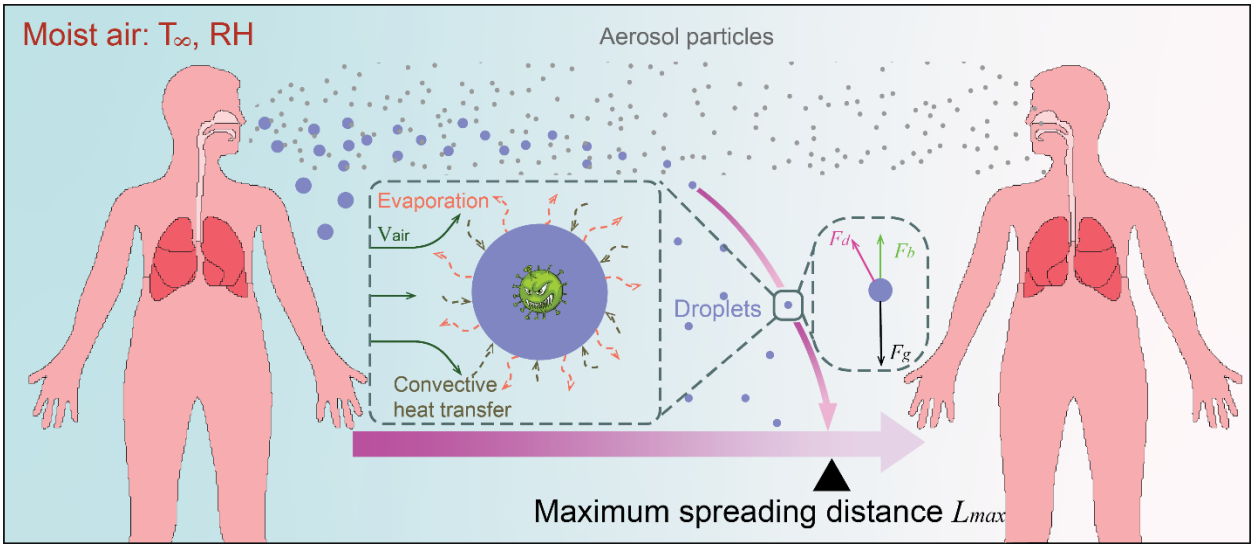

Figure 1. Transmission of COVID-19 through droplets and aerosol particles. After being exhaled by a patient, respiratory droplets with various sizes will travel and simultaneously evaporate in the ambient environment. Small-sized droplets dry immediately to form a cloud of aerosol particles. These particles will suspend in the air for a significant amount of time. Large-sized droplets can reach a limited distance and fall to the ground due to gravity. We define L_{max} as the maximum horizontal distance that droplets can travel before they either become dry aerosol particles or descend below the level of another person's hands, i.e., H/2 from the ground, where H is the height of another person.

To understand the evolution of respiratory droplets, we first examine a single respiratory droplet expelled from the URT of a patient. Upon being released, the droplet begins to exchange heat and mass with the environment while moving under various forces (gravity F_g, buoyancy F_b and air drag F_d in Figure 1). As described earlier, respiratory droplets will evolve into two categories depending on their initial diameter d_0: 1) *aerosol particles* made up of residues (salts, pathogens, enzymes, cells, and surfactants) after the dehydration of small droplets. Here we name those solid particles originating from small droplets as *aerosol particles* to distinguish from the airborne aerosol defined by the World Health Organization (WHO),(*36*) which employed a straight

5 μm cut-off. Generally, the aerosol particles in this study range from 1 μm to 10 μm and share similar dynamic behaviors and impact on human respiratory systems. Likewise, such virus-carrying aerosol particles can lead to airborne transmission of COVID-19 once being inhaled (*37, 38*). Because of their long suspension time in air, they have the potential of achieving long-range infection(*32*) Generally wearing a face mask can effectively lower the chance of transmission via aerosol particles. 2) *large droplets* that transmit the disease by contact. The infection range of these droplets is limited to a relatively short distance, because they are more sensitive to gravity and can settle on a surface before drying. If these droplets happen to land on the upper body of another person, viruses can easily enter their URTs by face-touching and eye-rubbing. This type of virus transmission can be prevented by practicing social distancing. We define a critical distance L_{max} as the maximum horizontal distance that all respiratory droplets can travel before they either shrink to suspending aerosol particles or descend to the level of another person's hands (H/2 from the ground, where H is the person's height). Beyond L_{max}, an individual will be completely clear of falling droplets (category 2), but can still be exposed to long-range aerosol particles (category 1), as shown in Figure 1.

The general modeling framework can be briefly summarized as: (1) the evaporation is a mass transport process dominated by the difference in the vapor pressure between the droplet surface and the ambient environment; (2) the temperature of the droplet is solved by considering heat transfer between the droplet and the environment via evaporation, radiation and convection; (3) gravity, buoyancy and drag contribute to the displacement of droplets/aerosol particles; (4) all thermophysical properties of the droplet and air are dependent on temperature and humidity. To improve upon previous models,(*23, 29, 35*) we further analyzed the effect of Brownian motion, considered the effect of residue salts in respiratory droplets on the terminal particle size, and incorporated a kinematic analysis on aerosol particle transport and deposition. We find that the Brownian motion becomes significant only for droplets with diameters smaller than 0.5 μm. The expected fluctuations of a 1 μm particle caused by Brownian motion is limited to 0.03 m in the life of a droplet. Therefore, we eventually neglected the Brownian force in formulating the kinematic equation. After complete evaporation of the droplets, the analysis on the residue aerosol particle was continued by solving its transport and deposition using kinematic equations. Detailed model formulations, including evaporation model, heat transfer model, kinematic analysis, and validations of our model can be found in the Supporting Information.

Key parameters considered in the model include the distribution of initial droplet size d_0, initial velocity v_0, environmental temperature T_∞, relative humidity RH, air velocity V_{air}, whose values are given here. The initial velocity v_0 of droplets was taken as 4.1 m/s for speaking.(*39*) We also calculated the sneezing mode (v_0=100 m/s) and the results are shown in the Supporting Information. For the subsequent sections, we choose to focus on speaking mode to mimic a real social distancing situation where people keep a reasonable physical distance and only sneeze/cough into a tissue or their elbow. The probability distribution of initial droplet diameter d_0 is from a previous experimental work by Duguid.(*40*), listed in the Supporting Information. The initial temperature T_0 of exhaled droplets was set to be 33 °C.(*41*) For the environment, we used an average V_{air} = 0.3 m/s in horizontal direction as the wind speed for an indoor environment,(*42*) and varied the wind speed from 0-3 m/s when analyzing the effect of ventilation and wind. In order to explore the effects of weather conditions, environmental temperature T_∞ and relative humidity RH were varied from 0-42 °C and 0-0.92, respectively.

We first characterize the dynamic behaviors of an individual respiratory droplet (T_0 = 33 °C) of different sizes d_0 produced by speaking (v_0 = 4.1 m/s) in typical indoor air (T_∞ = 23 °C, RH = 0.5 and V_{air} = 0.3 m/s). Figure S5(a) shows that the droplet diameter shrinks over time and that droplets smaller than 20 μm evaporate within 1 s. Figure S5(b) demonstrates that all the droplets cool to the wet bulb temperature T_{wb} in less than 1 second due to the latent heat required by evaporation. The trajectory of a droplet is analyzed in terms of the vertical distance L_z (Figure 2(a)) and horizontal distance L_x (Figure 2(b)) that the droplet can travel before it either completely dries or descends to the level of another person's hand (H/2). Here we set H to be the average height of American adults (1.75 m). Figure 2(a) shows that droplets with diameter smaller than 73.5 μm can completely dehydrate into aerosol particles and therefore only descend a vertical distance less than H/2. Droplets larger than 73.5 μm fall below the level of hands (H/2). They are less likely to transmit the disease and we do not consider them dangerous. Therefore, we used a plain cut-off of L_z = H/2 for all droplets falling below that. A critical droplet diameter d_c can be defined by identifying the initial diameter below which droplets can fully evaporate before descending to the hands. Figure 2(b) reveals that the maximum of L_x occurs at $d_0 = d_c$ as well. As shown in Figure 2(c), for $d<d_c$, L_x increases with respect to d_0 because a larger droplet takes longer time to fully

evaporate and thus travels further; as d exceeds d_c, the droplet falls more quickly due to gravity resulting in a smaller L_x.

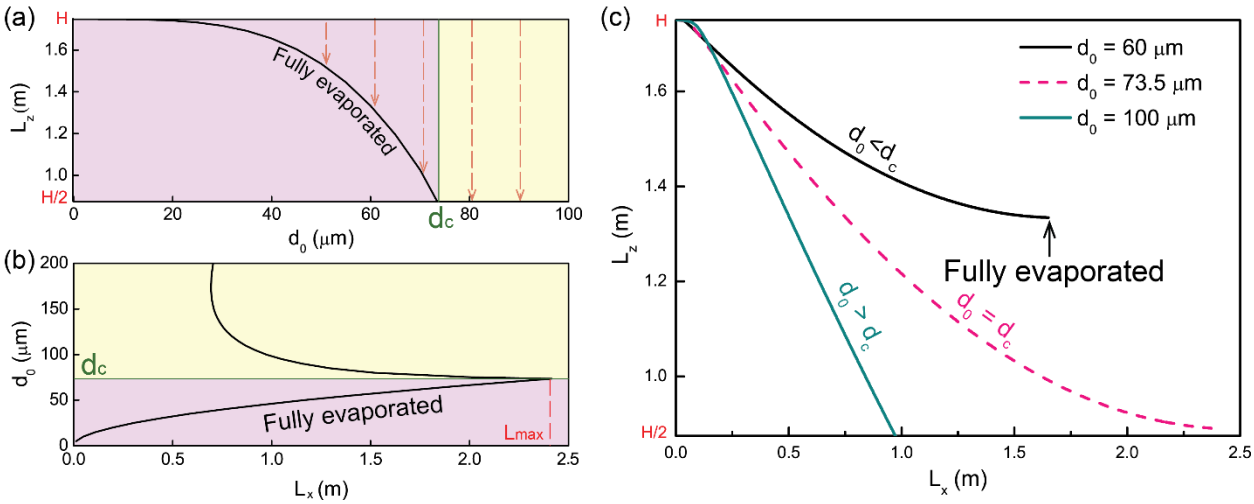

Figure 2. Model predictions of the trajectory of respiratory droplets. (a) The falling distance of respiratory droplets before completely drying out. (b) The horizontal traveling distance of respiratory droplets before drying or descending to the level of hands. (c) Trajectories of droplets with different initial diameters. The droplet has an initial temperature of T_0 = 33 °C and air conditions are T_∞ = 23 °C, RH = 0.5 and V_{air} = 0.3 m/s.

We then analyze the effect of weather conditions on the propagation of an ensemble of respiratory droplets in air (0.3 m/s) with an initial velocity of 4.1 m/s (speech mode). The results are presented in Figure 3. For droplet contact transmission, we plotted L_{max} as defined previously, under different temperature and humidity conditions (Figure 3a). It is shown that droplets can travel a longer distance in humid but cool environments, and therefore such environments require a longer social distance to completely eliminate droplet contact. In extremely cold and humid scenarios it can require as far as 6 m. On the other hand, respiratory droplets in hot and dry environments experience a faster mass loss as evaporation has been dramatically intensified. As those droplets sharply decrease in size, the horizontal traveling distance is reduced due to the growing damping effect of air. As a result, a less strict social distancing rule may potentially be applied on a really dry summer day, although at this point we have not examined the transmission via aerosol particles. We highlight that in most regions of Figure 3(a), L_{max} exceeds 1.8 m, i.e., the 6 feet of physical distance recommended by CDC. Therefore, current social distancing guidelines

may be insufficient in preventing all droplets from landing on an individual's upper body, especially for cold and humid environments.

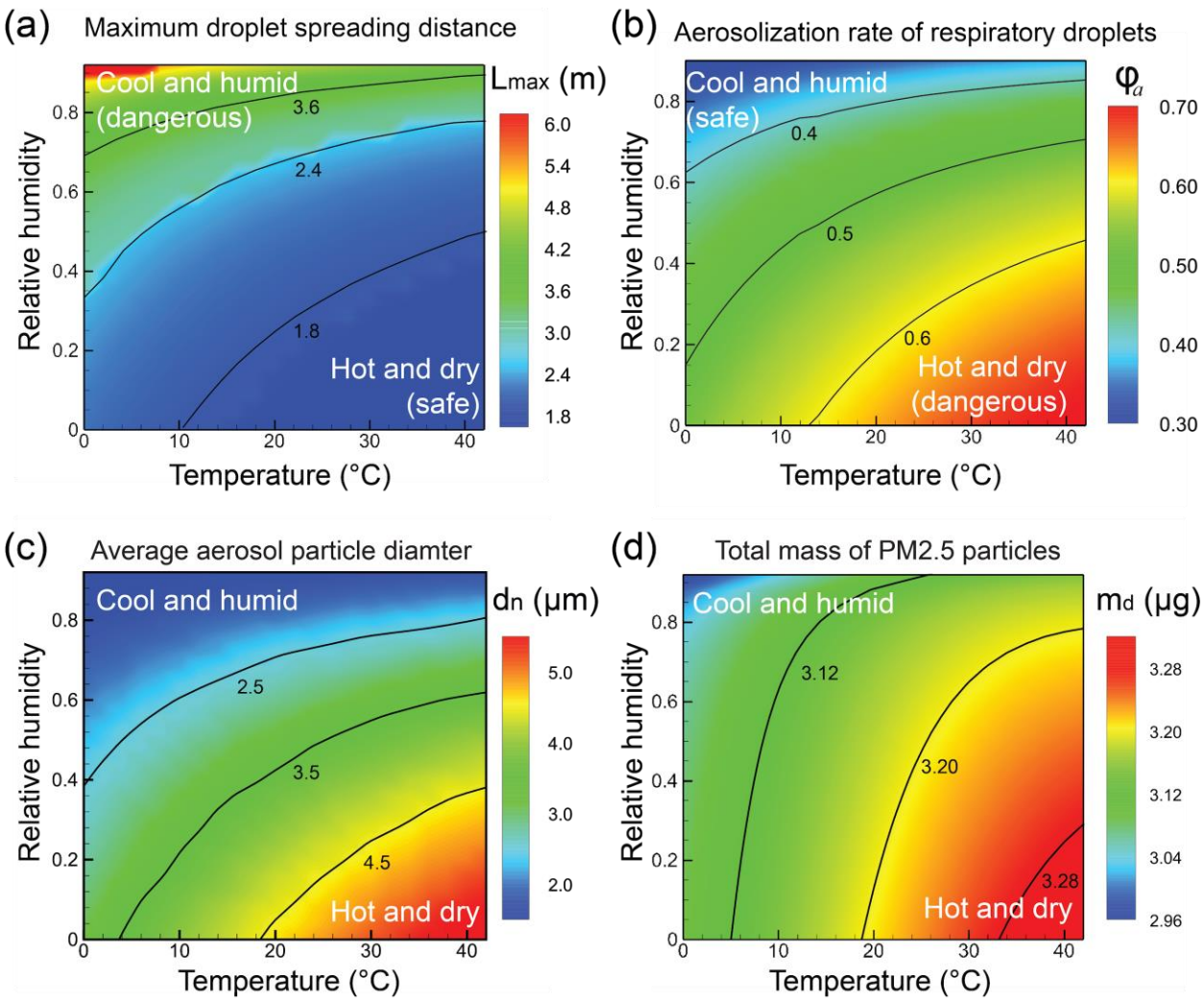

Figure 3. Effect of environmental factors on the transmission of COVID-19 via means of droplets contact and exposure to aerosol particles, respectively. (a) The maximum droplet traveling distance L_{max} under different weather conditions in terms of temperature and relative humidity. Droplets can reach a longer distance in a cool and humid environment. (b) Aerosolization rate φ_a, defined as the percentage of respiratory droplets turning into aerosol particles that can potentially travel beyond L_{max}, under different weather conditions in terms of temperature and humidity. (c) The average diameter of completely dry aerosol particles, under different weather conditions. (d) The total mass of PM2.5 floating in air that are produced by respiratory droplets per person at steady state in an enclosed space.

A quick remark regarding droplet-based transmission is that, if we consider a relaxed standard that only blocks 95% of viruses carried by respiratory droplets (excluding viruses carried by aerosol particles), this distance occurs at 1.4 m based on our model (Figure S5). Here we assumed a constant concentration of the virus in the droplets and the number of viruses is consequently proportional to the initial mass of respiratory droplets.(*43*) Interestingly, we find that this relaxed social distancing standard does not show an apparent dependence on the weather conditions (see Supporting Information). Therefore, 1.4 m may serve as a relaxed weather-independent criterion that can eliminate the majority of viruses from directly landing on another person. Caution is still required as this relaxed rule does not block transmission via aerosol particles and is evaluated for speaking mode with an air velocity of 0.3 m/s. The distance increases for an increased air velocity, the effect of which is discussed in a later section.

To further evaluate the potential risk of transmission of COVID-19 via aerosol particles, a mode that may be equally important,(*44*) we estimate the number of aerosolized particles, and elucidate the impact of environmental temperature and relative humidity. On the contrary to the trend observed for L_{max}, Figure 3(b) predicts an increasing aerosolization rate φ_a for hot and dry environments. φ_a is defined as the percentage of respiratory droplets that completely dehydrate before settling below the level of hands (H/2), and characterizes the amount of infectious aerosol particles that can be produced by speaking. The terminal sizes of these aerosol particles are in the range of 1 μm to 15 μm based on our model (Figure 3c and Figure S8). Such small particles can potentially suspend in air for hours (*28*, *37*) before settling (Figure S8) and tend to accumulate in public areas such as schools, offices, hotels, and hospitals. In particular, the increasing number of superspreading events that occurred at indoor environments evidenced the possibility of COVID-19 transmitting efficiently via aerosol particles. Therefore, the long-range infection induced by aerosol particles deserves more attention in the coming summer, especially in dry weather, since the resistivity of SARS-CoV-2 in these warm and dry environment is still not fully understood.(*30*, *32*)

The effectiveness of aerosol-based disease transmission is also linked to the ability of aerosol particles to infiltrate respiratory tracts, which has a strong particle size dependence. Generally, small particles are able to infiltrate lower in the respiratory tract to establish infections, as they can travel with inhaled air current and avoid impaction within the nasal region.(*24*) In

particular, studies have shown that PM2.5 (particles less than 2.5 μm in diameter) can penetrate deeply into our lungs,(*45*) which makes them potentially more dangerous than larger aerosol particles. Here we calculated the terminal size of an aerosol particle after dehydration by approximating it to the volume of sodium chloride originally dissolved in the aqueous solution. We assumed the respiratory droplet as a physiological saline solution (0.9% weight fraction),(*23*) when the composition of respiratory fluids is undoubtedly more complicated and can vary with respect to the site of origin, breathing pattern and health conditions of the host. We calculate the average diameter of aerosol particles floating in air under different weather conditions. Figure 3(c) demonstrates that aerosol particles have average diameters between 2-5 μm, and the maximum diameters are generally smaller than 10 μm, indicative of their strong ability to penetrate into the human respiratory system. The average particle diameter is increased for hot and dry weather, because more large droplets can completely evaporate due to enhanced evaporation (Figure 3b).

Since PM2.5 has been associated with a higher possibility of reaching the lung, we then discuss the transport and deposition of aerosol particles classified within PM2.5 under different weather conditions. We first computed the size-dependent suspension time t_s from the following equation:

$$v_e t_s + (v_t - v_e)\tau\left(1 - \exp\left(-\frac{t_s}{\tau}\right)\right) = \frac{L_m}{2} - L_z \quad (1)$$

where v_e is the falling velocity of the aerosol particle by assuming gravity is entirely balanced by buoyancy and air drag, v_t is the downward velocity of the aerosol particle at the time of drying out. If we neglect the Brownian motion, the time constant τ of the micro-sized droplet/particle can be written as (see Supporting Information for details):

$$\tau = \frac{2\rho_d r^2}{9\mu_a} \quad (2)$$

where ⊠$_d$ is the density of the droplet, r is the droplet radius and μ_a is the dynamic viscosity of air.

For respiratory droplets with diameters smaller than 100 μm, the time constant τ is less than 0.05 s, indicative of a strong damping effect of air. While large aerosol particles can suspend in air for at least 25 minutes, small aerosol suspends substantially longer (Figure S8(b)), which agrees with previous literature. (*22*) We further calculated the steady-state total mass m_d of PM2.5 produced by a patient in an enclosed and unventilated space. m_d is taken as the mass of PM2.5 when new

aerosol particles produced from speaking is balanced by their deposition onto the ground. Figure 3(d) presents the values of m_d in different environmental conditions. There is slightly more PM2.5 suspended in air in a hot and dry environment than in a cold and humid environment. This is mainly due to the increased suspension time in hot and dry environments as a result of the corresponding thermophysical properties of the air. By combining Figure 3(b) and (d), the hot and dry weather not only increases the percentage of respiratory droplets turning into aerosols, but also facilitates the accumulation of PM2.5 in an enclosed space. These facts raise a growing concern of aerosol transmission of COVID-19 in the coming summer, especially when the humidity is low.

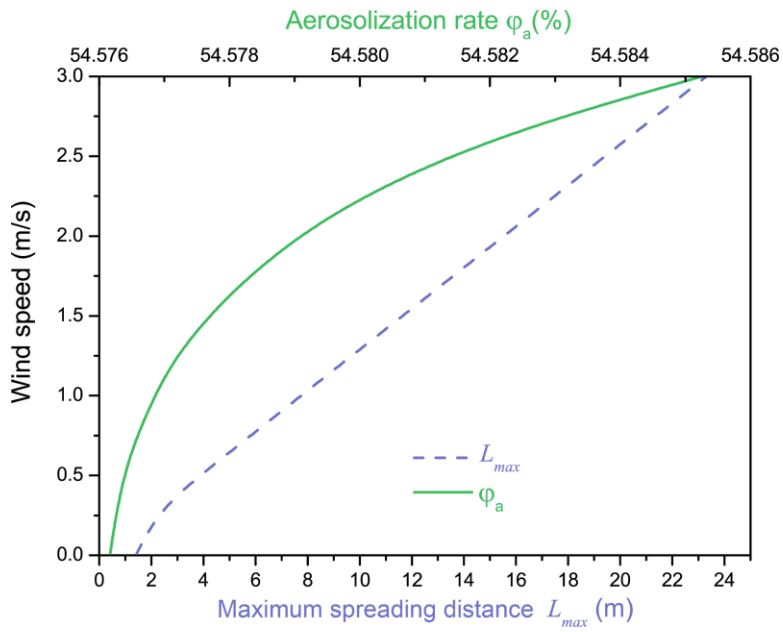

Figure 4. The effect of wind speed. Droplet spreading distance and aerosolization rate as a function of wind speed.

Ventilation is another environmental factor that plays a key role in the transmission of contagious diseases. There has been definitive and sufficient evidence to justify the connections between transmission of measles, tuberculosis, influenza and SARS and ventilating conditions in hospital.(*46*) However, there is still insufficient data regarding the ventilation requirements in other non-hospital public places, like schools, offices and cinemas.(*47*, *48*) Here, we investigate the effect of ventilation on the droplet spreading distance and aerosolization rate under a typical indoor environment (T_∞ = 23 °C, RH = 0.50). Different ventilation conditions are considered by changing the air speed from completely stagnant (V_{air} = 0 m/s), to a gentle breeze (V_{air} = 3 m/s).

To consider a worst situation, we model a scenario where the wind is always directed from an infected individual to a susceptible person. As shown in Figure 4, while the increased ventilation slightly affects the aerosolization rate of respiratory droplets, it has a significant impact on the spreading distance of droplets. The majority of droplets are moving with the airflow after their horizontal velocity settles down to the wind speed, which usually happens in a short time due to a small τ. Therefore, the droplet spreading distance has been dramatically increased as the wind velocity increases, with a maximum value of 23 m in a gentle breeze (V_{air} = 3 m/s). In addition, the spreading of aerosol particles is greatly increased as well, since they are smaller in size and travel with the wind. In summary, ventilation has both favorable and adverse consequences. While fresh outdoor air can effectively dilute the accumulation of infectious aerosol particles, it expands transport distances of pathogen-carrying droplets and aerosol particles. This poses stringent requirements on the meticulous design of ventilation configurations in non-hospital facilities, so as to cut off the transmission of COVID-19.

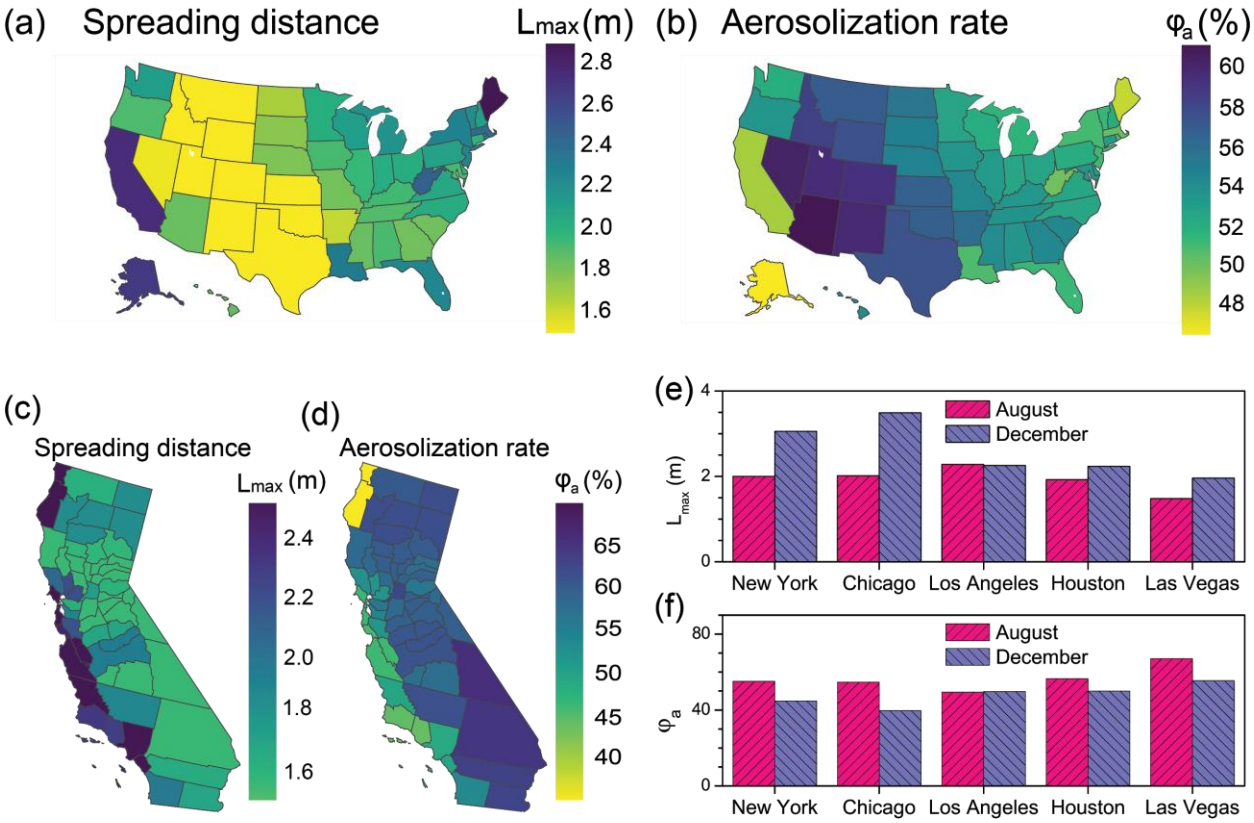

Figure 5. Geographical distribution of droplet spreading distance and aerosolization rate across the United States. (a) Spreading distance L_{max} and (b) aerosolization rate φ_a in each US state based on its monthly average weather condition in August. County-by-County distribution of (c) spreading distance L_{max} and (d) aerosolization rate φ_a in California based on their monthly average weather condition in August afternoon. (e) Safe distance L_{max} and (f) aerosolization rate φ_a in major US cities in summer and winter. Indoor wind speed is assumed (V_{air} = 0.3 m/s).

Finally, we compute the geographical distribution of spreading distance L_{max} and aerosolization rate φ_a across the United States to help evaluate the risk of infections caused by droplet contact and exposure to aerosol particles, which may provide the policymakers with a general guideline to curb the spread of this epidemic. Figure 5 (a) and (b) presents the state-by-state data based on the average weather conditions of each state in August.(*49*) Note that the weather data we collected are a monthly average over day and night as well as rural and urban regions. Generally, the inland regions are more vulnerable to aerosolization of viruses and the east and west coast should be cautious of droplet-based infections. California, on average, exhibits a higher risk of droplet spreading but a lower risk of infection induced by aerosol particles (Figure 5(a) and 5(b)). However, within the state of California, strong variations exist as shown in Figure 5(c) and 5(d). Note that Figure 5(c) and (d) were plotted using the average temperature and relative humidity in the afternoon of August.(*49*) The Mediterranean climate of California, together with the abundant oceanic moisture, brings the cool and moist summer for the coastal regions, which happens to be one of the most crowded regions in the US. Therefore, prolonged or more strict social distancing ought to be put into action to contain the virus. We also analyzed the anticipated disease transmission in major US cities in both summer (August) and winter (December) climates, as shown in Figure 5 (e) and (f). Compared to summer, there is a higher chance of droplet-based infections in winter, while the aerosolization rate merely changes. Considering the extreme stability of SARS-CoV-2 in low temperature,(*30*) a recurrent wintertime outbreak of COVID-19 is entirely probable.

Conclusions

In this study, we establish a comprehensive model which integrates emission of speech droplets, droplet evaporation, heat transfer and kinematic theories of droplet propagation to

provide a tentative answer to the controversial question of how weather conditions may affect the COVID-19 pandemic. When combined with systematic epidemiological studies, our results may shed light on the course of development of the current pandemic. The main findings of this study can be summarized as:

(1) Hot and dry weather can reduce infections caused by droplet contact, but the risk of transmission via aerosol particles is increased.
(2) Cool and humid weather can effectively suppress the formation of aerosol particles, but it also facilitates the spreading of large droplets.
(3) The current social distancing standard is insufficient in eliminating all droplet contacts. In some extremely cool and humid weathers, the required physical distance may reach as far as 6 m.
(4) Alternatively, a relaxed standard of 1.4 m is able to block 95% of viruses carried by respiratory droplets (excluding that carried by aerosol particles) and shows negligible weather dependence.
(5) There is a slight increase of PM2.5 floating in air in hot and dry weather, owing to the increased suspension time.
(6) Improper design of ventilation systems can dramatically increase the traveling distance of both droplets and aerosol particles, and consequently increases the likelihood of infections in both modes.

The messages to the general public and authorities that we can derive from our model results are listed.

(1) The current pandemic may not ebb in the upcoming summer in the northern hemisphere. More data on the infectivity of SARS-CoV-2 under different weather conditions, especially in the form of aerosol particles, are necessary to make a definitive conclusion.
(2) Measures should be taken to contain COVID-19 transmission caused by aerosol particles in summer, especially when humidity is low. Proper face-covering may serve as a solution to prevent infectious PM2.5 and PM10 from entering our respiratory tracts. (*50*)
(3) The effect of weather on the transmission of COVID-19 is not monotonic. Adaptable strategies by incorporating the regionality, weather and modes of transmission should be applied to contain the transmission.

(4) More attention should be given to the optimization of building ventilation systems. A proper design of ventilation systems by directing wind away from people and preventing mixing of airflow in a public area can vastly reduce both droplet contacts and exposure to aerosol particles.

However, our study is still subject to a number of limitations. Firstly, our model predicts how far respiratory droplets can travel under different environmental conditions, and should be combined with infectivity studies of SARS-CoV-2 under all weather conditions. As there is an ongoing debate on the activity of SARS-CoV-2 under different temperature, humidity and sunlight conditions, further studies are necessary to quantify the infectivity variations of SARS-CoV-2 and integrate them in the current model. Secondly, the dynamics of droplets are assumed to be independent on other droplets. Recent works demonstrate that a turbulent gas cloud can be produced with exhalation, which entrains the droplet and suppress its evaporation.(*20*) To address this issue, computational fluid dynamics (CFD) simulations of the multiphase turbulent cloud can be used to explore the interactions between droplet and cloud, cloud and the environment, as well as droplet and the environment. However, it is beyond the scope of current study. Thirdly, the composition of a respiratory droplet is complicated and we modeled it as the physiological saline solution. The effect of droplet composition on the activities of SARS-CoV-2 as the droplet evaporates warrants further research.

REFERENCES

1. E. Dong, H. Du, L. Gardner, An interactive web-based dashboard to track COVID-19 in real time. *Lancet Infect. Dis.* **20**, 533–534 (2020).
2. P. Zhou, X.-L. Yang, X.-G. Wang, B. Hu, L. Zhang, W. Zhang, H.-R. Si, Y. Zhu, B. Li, C.-L. Huang, others, A pneumonia outbreak associated with a new coronavirus of probable bat origin. *nature*. **579**, 270–273 (2020).
3. F. Wu, S. Zhao, B. Yu, Y.-M. Chen, W. Wang, Z.-G. Song, Y. Hu, Z.-W. Tao, J.-H. Tian, Y.-Y. Pei, others, A new coronavirus associated with human respiratory disease in China. *Nature*. **579**, 265–269 (2020).
4. W. Guan, Z. Ni, Y. Hu, W. Liang, C. Ou, J. He, L. Liu, H. Shan, C. Lei, D. S. Hui, others, Clinical characteristics of coronavirus disease 2019 in China. *N. Engl. J. Med.* **382**, 1708–1720 (2020).
5. M. Letko, A. Marzi, V. Munster, Functional assessment of cell entry and receptor usage for SARS-CoV-2 and other lineage B betacoronaviruses. *Nat. Microbiol.* **5**, 562–569 (2020).
6. K. Leung, J. T. Wu, D. Liu, G. M. Leung, First-wave COVID-19 transmissibility and severity in China outside Hubei after control measures, and second-wave scenario planning: a modelling impact assessment. *The Lancet* (2020).

7. M. Gandhi, D. S. Yokoe, D. V. Havlir, *Asymptomatic transmission, the Achilles' heel of current strategies to control COVID-19* (Mass Medical Soc, 2020).
8. M. M. Arons, K. M. Hatfield, S. C. Reddy, A. Kimball, A. James, J. R. Jacobs, J. Taylor, K. Spicer, A. C. Bardossy, L. P. Oakley, others, Presymptomatic SARS-CoV-2 infections and transmission in a skilled nursing facility. *N. Engl. J. Med.* (2020).
9. C. Rothe, M. Schunk, P. Sothmann, G. Bretzel, G. Froeschl, C. Wallrauch, T. Zimmer, V. Thiel, C. Janke, W. Guggemos, others, Transmission of 2019-nCoV infection from an asymptomatic contact in Germany. *N. Engl. J. Med.* **382**, 970–971 (2020).
10. J. Yuan, M. Li, G. Lv, Z. K. Lu, Monitoring transmissibility and mortality of COVID-19 in Europe. *Int. J. Infect. Dis.* (2020).
11. A. Pan, L. Liu, C. Wang, H. Guo, X. Hao, Q. Wang, J. Huang, N. He, H. Yu, X. Lin, Association of public health interventions with the epidemiology of the COVID-19 outbreak in Wuhan, China. *Jama* (2020).
12. Y. Liu, A. A. Gayle, A. Wilder-Smith, J. Rocklöv, The reproductive number of COVID-19 is higher compared to SARS coronavirus. *J. Travel Med.* (2020).
13. T. V. Inglesby, Public Health Measures and the Reproduction Number of SARS-CoV-2. *JAMA* (2020).
14. G. Chowell, C. Castillo-Chavez, P. W. Fenimore, C. M. Kribs-Zaleta, L. Arriola, J. M. Hyman, Model Parameters and Outbreak Control for SARS. *Emerg. Infect. Dis.* **10**, 1258–1263 (2004).
15. T. F. Booth, B. Kournikakis, N. Bastien, J. Ho, D. Kobasa, L. Stadnyk, Y. Li, M. Spence, S. Paton, B. Henry, others, Detection of airborne severe acute respiratory syndrome (SARS) coronavirus and environmental contamination in SARS outbreak units. *J. Infect. Dis.* **191**, 1472–1477 (2005).
16. S. Herfst, E. J. Schrauwen, M. Linster, S. Chutinimitkul, E. de Wit, V. J. Munster, E. M. Sorrell, T. M. Bestebroer, D. F. Burke, D. J. Smith, others, Airborne transmission of influenza A/H5N1 virus between ferrets. *science*. **336**, 1534–1541 (2012).
17. E. C. Cole, C. E. Cook, Characterization of infectious aerosols in health care facilities: an aid to effective engineering controls and preventive strategies. *Am. J. Infect. Control*. **26**, 453–464 (1998).
18. V. Stadnytskyi, C. E. Bax, A. Bax, P. Anfinrud, The airborne lifetime of small speech droplets and their potential importance in SARS-CoV-2 transmission. *Proc. Natl. Acad. Sci.* (2020).
19. X. Xie, Y. Li, H. Sun, L. Liu, Exhaled droplets due to talking and coughing. *J. R. Soc. Interface*. **6**, S703–S714 (2009).
20. L. Bourouiba, Turbulent Gas Clouds and Respiratory Pathogen Emissions: Potential Implications for Reducing Transmission of COVID-19. *JAMA.* **323**, 1837–1838 (2020).
21. R. Mittal, R. Ni, J.-H. Seo, The flow physics of COVID-19. *J. Fluid Mech.* **894** (2020), doi:10.1017/jfm.2020.330.
22. B. E. Scharfman, A. H. Techet, J. W. M. Bush, L. Bourouiba, Visualization of sneeze ejecta: steps of fluid fragmentation leading to respiratory droplets. *Exp. Fluids*. **57**, 24 (2016).
23. X. Xie, Y. Li, A. Chwang, P. Ho, W. Seto, How far droplets can move in indoor environments–revisiting the Wells evaporation-falling curve. *Indoor Air*. **17**, 211–225 (2007).
24. J. Gralton, E. Tovey, M.-L. McLaws, W. D. Rawlinson, The role of particle size in aerosolised pathogen transmission: A review. *J. Infect.* **62**, 1–13 (2011).
25. K. A. Kormuth, K. Lin, A. J. Prussin, E. P. Vejerano, A. J. Tiwari, S. S. Cox, M. M. Myerburg, S. S. Lakdawala, L. C. Marr, Influenza virus infectivity is retained in aerosols and droplets independent of relative humidity. *J. Infect. Dis.* **218**, 739–747 (2018).

26. M. Nicas, D. Best, A study quantifying the hand-to-face contact rate and its potential application to predicting respiratory tract infection. *J. Occup. Environ. Hyg.* **5**, 347–352 (2008).
27. M. Nicas, G. Sun, An Integrated Model of Infection Risk in a Health-Care Environment. *Risk Anal.* **26**, 1085–1096 (2006).
28. R. Tellier, Aerosol transmission of influenza A virus: a review of new studies. *J. R. Soc. Interface*. **6**, S783–S790 (2009).
29. W. Wells, ON AIR-BORNE INFECTION: STUDY II. DROPLETS AND DROPLET NUCLEI. *Am. J. Epidemiol.* **20**, 611–618 (1934).
30. A. Chin, J. Chu, M. Perera, K. Hui, H.-L. Yen, M. Chan, M. Peiris, L. Poon, Stability of SARS-CoV-2 in different environmental conditions. *Lancet Microbe*. **1**, e10 (2020).
31. N. van Doremalen, T. Bushmaker, D. H. Morris, M. G. Holbrook, A. Gamble, B. N. Williamson, A. Tamin, J. L. Harcourt, N. J. Thornburg, S. I. Gerber, Aerosol and surface stability of SARS-CoV-2 as compared with SARS-CoV-1. *N. Engl. J. Med.* **382**, 1564–1567 (2020).
32. A. C. Fears, W. B. Klimstra, P. Duprex, A. Hartman, S. C. Weaver, K. S. Plante, D. Mirchandani, J. Plante, P. V. Aguilar, D. Fernandez, others, Comparative dynamic aerosol efficiencies of three emergent coronaviruses and the unusual persistence of SARS-CoV-2 in aerosol suspensions. *medRxiv* (2020).
33. J. Wang, K. Tang, K. Feng, W. Lv, High temperature and high humidity reduce the transmission of COVID-19. *Available SSRN 3551767* (2020).
34. S. M. Kissler, C. Tedijanto, E. Goldstein, Y. H. Grad, M. Lipsitch, Projecting the transmission dynamics of SARS-CoV-2 through the postpandemic period. *Science* (2020).
35. J. Kukkonen, T. Vesala, M. Kulmala, The interdependence of evaporation and settling for airborne freely falling droplets. *J. Aerosol Sci.* **20**, 749–763 (1989).
36. W. H. Organization, *Infection prevention and control of epidemic-and pandemic-prone acute respiratory infections in health care* (World Health Organization, 2014).
37. M. Alsved, L. Bourouiba, C. Duchaine, J. Löndahl, L. C. Marr, S. T. Parker, A. J. Prussin, R. J. Thomas, Natural sources and experimental generation of bioaerosols: Challenges and perspectives. *Aerosol Sci. Technol.* **54**, 547–571 (2020).
38. S. Poulain, L. Bourouiba, Disease transmission via drops and bubbles. *Phys. Today*. **72**, 70–71 (2019).
39. S.-B. Kwon, J. Park, J. Jang, Y. Cho, D.-S. Park, C. Kim, G.-N. Bae, A. Jang, Study on the initial velocity distribution of exhaled air from coughing and speaking. *Chemosphere*. **87**, 1260–1264 (2012).
40. J. P. Duguid, The size and the duration of air-carriage of respiratory droplets and droplet-nuclei. *Epidemiol. Infect.* **44**, 471–479 (1946).
41. P. Höppe, Temperatures of expired air under varying climatic conditions. *Int. J. Biometeorol.* **25**, 127–132 (1981).
42. P. E. Baldwin, A. D. Maynard, A survey of wind speeds in indoor workplaces. *Ann. Occup. Hyg.* **42**, 303–313 (1998).
43. E. P. Vejerano, L. C. Marr, Physico-chemical characteristics of evaporating respiratory fluid droplets. *J. R. Soc. Interface*. **15**, 20170939 (2018).
44. P. Bahl, C. Doolan, C. de Silva, A. A. Chughtai, L. Bourouiba, C. R. MacIntyre, Airborne or droplet precautions for health workers treating COVID-19? *J. Infect. Dis.* (2020).
45. Y.-F. Xing, Y.-H. Xu, M.-H. Shi, Y.-X. Lian, The impact of PM2. 5 on the human respiratory

system. *J. Thorac. Dis.* **8**, E69 (2016).
46. J. G. Cedeño-Laurent, A. Williams, P. MacNaughton, X. Cao, E. Eitland, J. Spengler, J. Allen, Building Evidence for Health: Green Buildings, Current Science, and Future Challenges. *Annu. Rev. Public Health*. **39**, 291–308 (2018).
47. Y. Li, G. M. Leung, J. W. Tang, X. Yang, C. Y. Chao, J. Z. Lin, J. W. Lu, P. V. Nielsen, J. Niu, H. Qian, Role of ventilation in airborne transmission of infectious agents in the built environment-a multidisciplinary systematic review. *Indoor Air*. **17**, 2–18 (2007).
48. Z. T. Ai, T. Huang, A. K. Melikov, Airborne transmission of exhaled droplet nuclei between occupants in a room with horizontal air distribution. *Build. Environ.* **163**, 106328 (2019).
49. Weather Averages for the United States, (available at https://www.currentresults.com/Weather/US/weather-averages-index.php).
50. L. Liao, W. Xiao, M. Zhao, X. Yu, H. Wang, Q. Wang, S. Chu, Y. Cui, Can N95 Respirators Be Reused after Disinfection? How Many Times? *ACS Nano* (2020).

SUPPORTING INFORMATION

COVID-19: Effects of weather conditions on the propagation of respiratory droplets

Lei Zhao[1], Yuhang Qi[1], Paolo Luzzatto-Fegiz[1], Yi Cui[2,3], Yangying Zhu[1*]

[1]Department of Mechanical Engineering, University of California Santa Barbara, Santa Barbara CA, USA

[2]Department of Materials Science and Engineering, Stanford University, Stanford, CA, USA

[3]Stanford Institute for Materials and Energy Sciences, SLAC National Accelerator Laboratory, Menlo Park, CA, USA

*To whom correspondence should be addressed

Yangying Zhu, Email: yangying@ucsb.edu

Model Formulations

When a droplet with an initial diameter of d_0 and temperature T_0 is moving in air with temperature T_∞ and relative humidity RH, the evaporative flux of the droplet is determined by the difference of vapor pressure near the droplet surface p_{vs} and of the ambient environment $p_{v\infty}$. (*1*, *2*)

$$\frac{dm_p}{dt} = \frac{2\pi d M_v D_\infty}{RT_\infty} \cdot C \cdot Sh \cdot \ln\left(\frac{p - p_{vs}}{p - p_{v\infty}}\right) \tag{S1}$$

where m_p is the mass of the droplet, t is the time, d is the diameter of the droplet, M_v is the molecular mass of the droplet, D_∞ is the binary diffusion coefficient of the air, *R* is the universal gas constant and p is the total pressure of the air. *C* is the correction factor due to temperature dependence of diffusion coefficient.(*3*)

$$C = \frac{T_\infty - T}{T_\infty^{\lambda - 1}} \frac{2 - \lambda}{T_\infty^{2-\lambda} - T^{2-\lambda}} \tag{S2}$$

where T is the temperature of the droplet and λ is a constant specifically for water. *Sh* is the Sherwood number.

$$Sh = 1 + 0.3 Re^{\frac{1}{2}} Sc^{\frac{1}{3}} \tag{S3}$$

Re and Sc are the Reynolds number and Schmidt number, which can be calculated as:

$$Re = \frac{\rho_a \left(V - V_{air}\right) d}{\mu}, \; Sc = \frac{\mu}{\rho_a D_\infty} \tag{S4}$$

where ⊠$_a$ is the density of the air, V_{air} is the wind speed, V is the droplet velocity and μ is the dynamic viscosity of the air.

p_{vs} is the vapor pressure at the droplet surface and is lowered by the dissolved substances in its solution, which can be described by the Raoult's law $p_{vs} = f_w p_{v0}(T)$, where f_w is the mole fraction of water in the solution and p_{v0} is the saturation vapor pressure at temperature T. The composition of a respiratory droplet can be extremely complex and may contain pathogens, proteins, salt, and surfactants. In this study, we assume the respiratory droplet as a physiological saline solution with 0.9% weight fraction of sodium chloride. During the evaporation process, sodium chloride begins to precipitate once the saturating concentration has been reached. The as-

formed NaCl crystal will serve as a nest where SARS-CoV-2 can reside. Its diameter d_r after dry-out can be calculated as:

$$d_r = \left(\frac{6m_s}{\pi\rho_s}\right)^{\frac{1}{3}} \tag{S5}$$

where m_s is the mass of NaCl initially dissolved in the droplet and ρ_s is the density of NaCl crystal.

The heat transfer between the droplet and the air is dominated by evaporation, convection, and radiation. An energy balance equation can be derived as:

$$m_p c_p \frac{dT}{dt} = 2\pi d k_a \left(T_\infty - T\right) \cdot Nu + L_v \frac{dm_p}{dt} + \pi d^2 \Gamma \left(T_\infty^4 - T^4\right) \tag{S6}$$

where c_p is the specific heat capacity of the droplet, k_a is the thermal conductivity of the air, L_v is the latent heat of vaporization and Γ is the Stefan–Boltzmann constant. Nu is the Nusselt number.

$$Nu = 1 + 0.3 Re^{\frac{1}{2}} Pr^{\frac{1}{3}} \tag{S7}$$

$Pr = \frac{c_a \mu}{k_a}$ is the Prandtl number, where c_a is the specific heat capacity of the air.

The displacement of velocity of the droplet can be calculated by considering gravity, buoyancy and air drag as the dominating factors.

$$m_p \frac{d\vec{V}}{dt} = m_p \vec{g}\left(1 - \frac{\rho_a}{\rho}\right) - \frac{1}{2}\frac{\pi d^2}{4} C_d \rho_a \left|\vec{V} - \vec{V}_{air}\right| \left(\vec{V} - \vec{V}_{air}\right) + F_B \tag{S8}$$

where $\vec{g}$ is the gravity and ρ is the density of the droplet. C_d is the drag coefficient, which can be determined by the following equation.

$$C_d = \begin{cases} 0.424 & Re > 1000 \\ \frac{24}{Re}\left(1 + \frac{1}{6} Re^{\left(\frac{2}{3}\right)}\right) & Re \leq 1000 \end{cases} \tag{S9}$$

F_B is the random Brownian force, which will be discussed in the next section.

In this study, moist air is used to calculate the dependence of gas properties on RH. Those temperature dependent parameters are taken from Kukkonen et al. (1989).(*2*)

All simulations of droplets were stopped if 1) the droplet has completely dehydrated, i.e., $d \leq d_r$, where d_r is the diameter of droplet nuclei formed by residues; or 2) the droplet has descended to the level of another person's hands, i.e., $|L_z| \geq H/2$, where L_z is the vertical displacement.

Effect of Brownian Motion

Most respiratory droplets are smaller than 100 µm. Once they dry out, the droplet nuclei that are left behind are usually smaller than 10 µm. Therefore, the movement of such particles becomes sensitive to impacts from fast moving air molecules, which poses a random component F_B in the kinematic equation, as presented in equation S8. F_B is supposed to vary extremely rapidly over the time of any observation. The effect of the fluctuating force can be summarized by giving its first and second moments:

$$\langle F_B(t) \rangle = 0, \ \langle F_B(t_1) F_B(t_2) \rangle = 2\beta k_B T \delta(t_1 - t_2) \tag{S10}$$

The average $\langle \cdots \rangle$ is an average with respect to the distribution of the realizations of the stochastic variable $F_B(t)$. The delta function $\delta(t_1 - t_2)$ in time indicates that there is no correlation between impacts in any distinct time intervals t_1 and t_2. β is the damping coefficient and can be derived from the Einstein relation.

$$\beta = 3\pi\mu d \tag{S11}$$

The fluctuating force F_B has a Gaussian distribution with the moments specified in equation S10. Therefore, the effect of Brownian force F_B can be estimated by comparing it to the gravity.

$$\frac{F_B}{m_p g} = \frac{\sqrt{2\beta k_B T}}{\frac{1}{6}\pi d^3 \rho} \tag{S12}$$

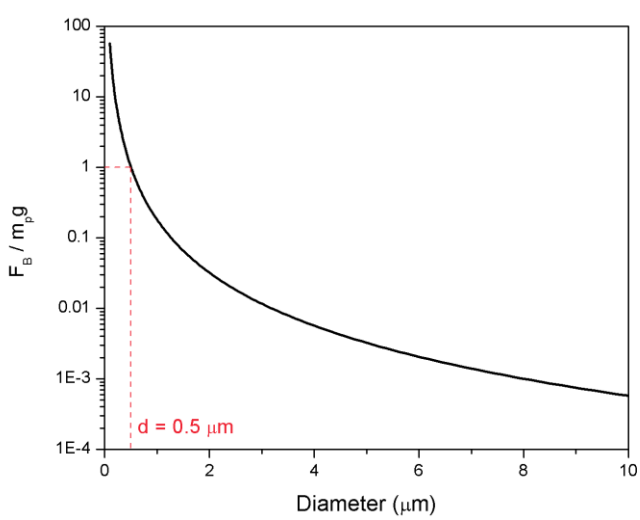

Figure S1. Effect of Brownian force at different length scales

Figure S1 presents the comparison of F_B to gravity at different nuclei diameters. It is found that the Brownian force F_B is comparable to gravity only if the nuclei size becomes smaller than 0.5 μm. In this case, the corresponding initial diameter of the droplet calculated from equation S5 must be smaller than 3.4 μm. However, respiratory droplets are larger than 5 μm according to previous measurements. (*4*)

The effect of Brownian force on the movement of droplet nuclei can be accounted for in an alternative way. Assuming that the droplet nuclei are at equilibrium in that gravity equals to the air drag, then the motion of those nuclei become purely diffusive and the dependent displacement can be described as:

$$\Delta x(t) = \int_0^t V^*(t')\,\mathrm{d}t' \tag{S13}$$

where V* is the fluctuating velocity resulting from the random Brownian force. The time-averaged displacement $\overline{\Delta x}$ is equal to 0, but the mean square displacement $\langle \Delta x(t)^2 \rangle$ can be evaluated as:

$$\langle \Delta x(t)^2 \rangle = 2Dt = \frac{2k_B T}{3\pi\mu d} t \tag{S14}$$

Therefore, the average deviation of droplet nuclei in a duration of t is:

$$\langle |\Delta x(t)| \rangle = \sqrt{\frac{2k_B T}{3\pi\mu d_r} t} \tag{S15}$$

where d_r is the diameter of the droplet nucleus. For T = 300K and d_r = 1 μm um, we find that its expected moving distance is only 0.03 m in 5000 seconds, which is negligible in the transmission of both aerosol particles and droplets.

To conclude, we find that the effect of Brownian motion on the transmission of respiratory droplets and droplet nuclei is negligible, in that 1) the fluctuating Brownian force is trivial compared to the gravity for the size of interest (d > 1 μm); 2) the deviation of those particles from their original induced by Brownian motion is negligible.

Model Validations

To validate our model, we firstly investigated the evaporation of stagnant water droplets (T_0 = 9 °C) evaporating in dry air (T_∞ = 25 °C, RH = 0) and compared the results to an experimental work by Ranz and Marshall.(*5*) As shown in Figure S2 (a), our results are in excellent agreement with the experimental data.

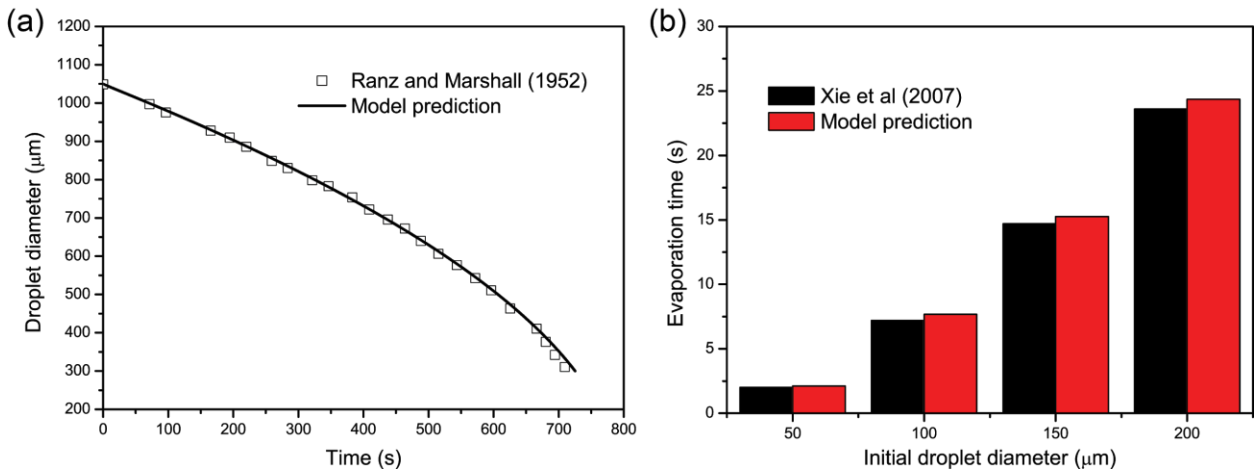

Figure S2. Comparison of model predictions to (a) Ranz and Marshall (1952) and (b) Xie et al. (2007)

Then we also studied the process of evaporation of a falling droplet (T_0 = 33 °C) in dry air (T_∞ = 25 °C, RH = 0) and compared to Xie et al (2007) in Figure S2 (b). Generally, our results agree well with Xie et al (2007) and the overshoot of our model results may be attributed to the small differences in water and air parameters that were adopted.

Size and Distribution of Speech Droplets

The size and distribution of speech droplets, i.e., respiratory droplets expelled by speaking, are taken from a work published by J. P, Duguid.(*4*) Here we present a probability density distribution of different initial diameters of speech droplets in Figure S3.

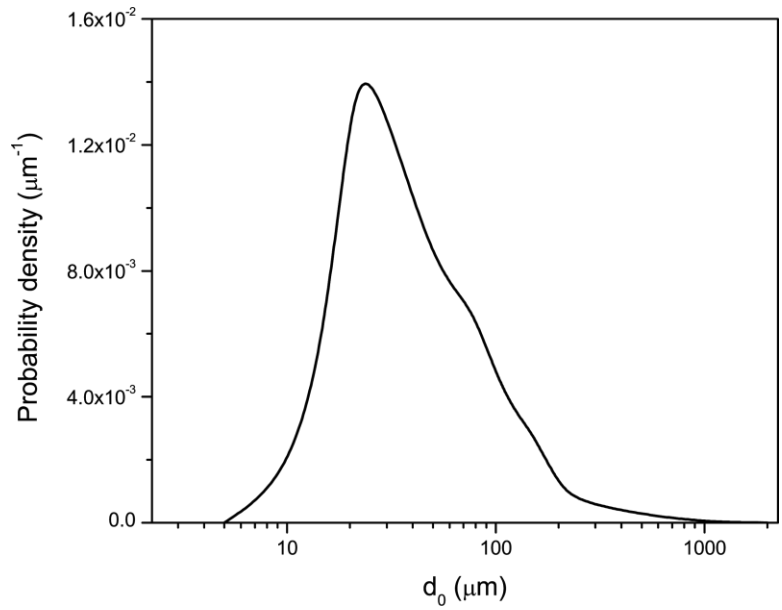

Figure S3. Probability density distribution of the initial diameter of speech droplets

Kinematic Analysis of Aerosol Transport

Once the droplet has dried out, as-formed aerosol particles will suspend in air for a long time and eventually fall on the ground due to gravity. If there is no airflow in vertical direction, the vertical movement of aerosol particles is solely controlled by gravity, buoyancy and air drag. Because the downward velocity v_z of droplet nuclei are usually on the order of 10^{-5}-10^{-4} m/s, Re<<1 and therefore we can assume a Stokes flow around the droplet nuclei.

$$m_r \frac{dv_z}{dt} = m_r g\left(1 - \frac{\rho_a}{\rho}\right) - 6\pi\mu r v_z \tag{S16}$$

where m_r is the mass and r is the radius of the droplet nucleus. Equation S16 can be solved with initial condition of $v_z = v_0$ at t = 0, where v_t is the terminal velocity of the droplet.

$$v_z = (v_t - v_e)e^{-\frac{t}{\tau}} + v_e \tag{S17}$$

τ is the time constant.

$$\tau = \frac{m_r}{6\pi\mu R} = \frac{2\rho r^2}{9\mu} \tag{S18}$$

$v_e = g\tau(1-\rho_a/\rho)$ is the falling velocity of the aerosol particle by assuming gravity is entirely balanced by buoyancy and air drag.

Evaporation dynamics of droplets

We first examine the evaporation dynamics of a sneezing droplet (T_0 = 33 °C, v_0 = 100 m/s) in T_∞ = 20 °C and RH = 0.4. The time-dependent characteristics of an evaporating sneezing droplet is shown in Figure S4.

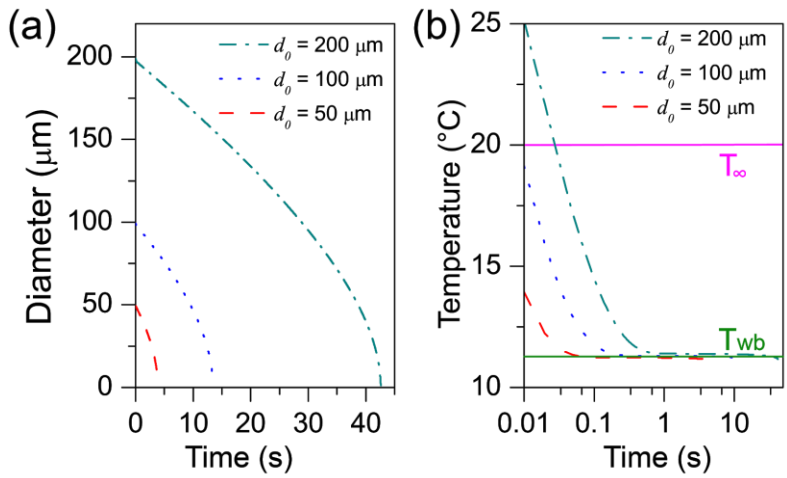

Figure S4. Evolution of (a) droplet diameter and (b) droplet temperature of a sneezing droplet. The initial condition of the droplet is taken as T_0 = 33 °C and v_0 = 100 m/s. The environment is set to be T_∞ = 20 °C, RH = 0.4 and V_{air} = 0 m/s.

Figure S4 demonstrates the strong dependence of droplet evaporation dynamics on the initial diameter of a sneezing droplet. In Figure S4(a), the diameter of a small droplet (d_0 = 50 μm) experiences a rapid decrease. For a large droplet, the diameter firstly decreases linearly, because the evaporative flux at this point is primarily determined by the vapor pressure difference; eventually its diameter experiences a sharp decrease in that the increasing surface-to-volume ratio further intensifies the evaporation. Figure S4(b) presents the temperature profile of a droplet during evaporation. Note that the x axis in this figure is in logarithmic scale. Apparently, the temperature of all droplets rapidly decreases to the wet bulb temperature T_{wb} within one second, owing to the large latent heat required to evaporate. Therefore, the effect of heat transfer is not significant on the evaporation dynamics, as the droplet stays at T_{wb} throughout the evaporation process.

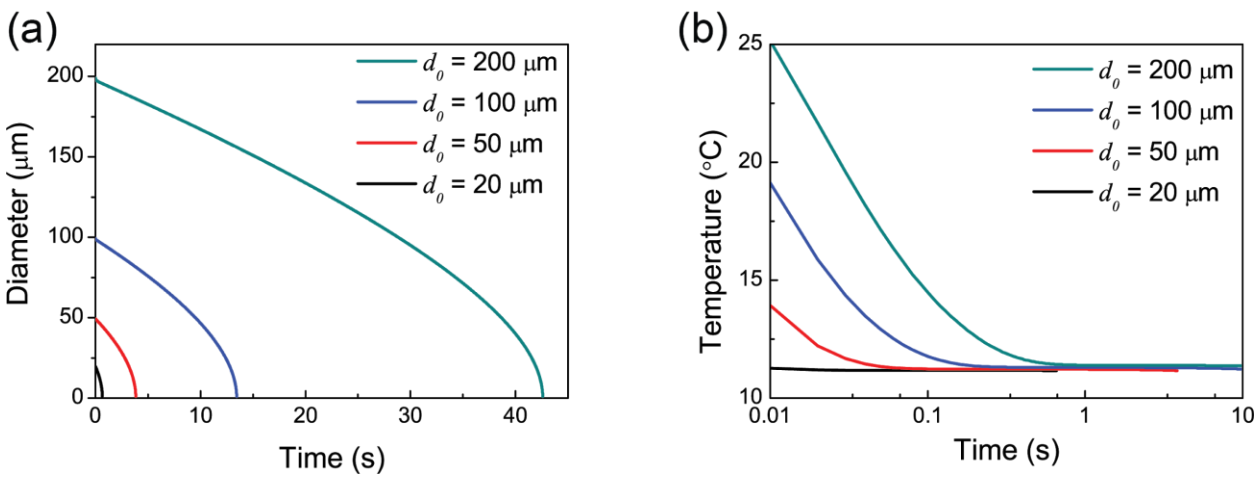

Figure S5. Evolution of (a) droplet diameter and (b) droplet temperature of a speech droplet. The initial condition of the droplet is taken as T_0 = 33 ℃ and v_0 = 4.1 m/s. The environment is set to be T_∞ = 23 ℃, RH = 0.5 and V_{air} = 0.3 m/s.

Figure S5 shows the evaporation dynamics of a speech droplet that has a smaller initial velocity. The environment is taken as the typical indoor air, i.e., T_∞ = 23 ℃, RH = 0.5 and V_{air} = 0.3 m/s. Generally, the speech droplet shares the similar behaviors with the sneezing droplet, as the respiratory droplets are sensitive to air drag and its velocity can decelerate to the wind velocity rapidly.

Viral load in respiratory droplets

If the concentration of SARS-CoV-2 is constant in all respiratory secretions, then the number of viruses N_v in a respiratory droplet is determined by its size.

$$N_v = \frac{\pi n d_0^3}{6} \tag{S19}$$

where n is the average number per unit volume. Based on the size distribution presented in Figure S3 and J. P, Duguid(*4*), we calculated the percentage of viral load in each diameter range (Figure S6 (a)).

$$\xi(d_0) = \frac{N_v(d_0)}{\sum_{d_0} N_v} \tag{S20}$$

We find that almost 96% of viruses produced by one expiration are carried in droplets with d_0 > 200 μm. Therefore, the droplet contact transmission could be surprisingly dangerous.

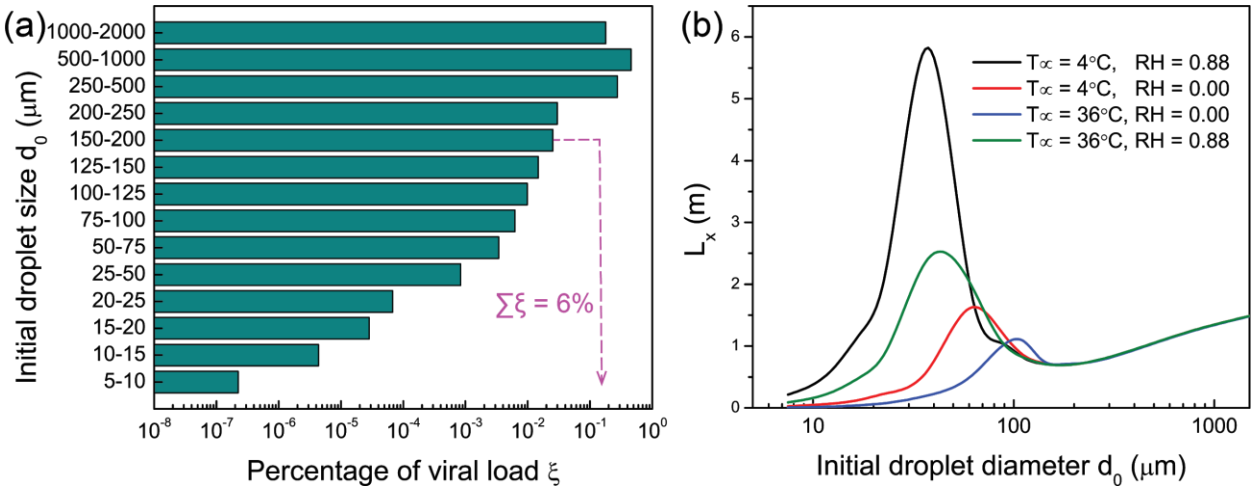

Figure S6. (a) Viral load distribution over different initial droplet size d_0. (b) Spreading distance L_x for droplets with different initial diameter d_0.

In order to obtain the distance-dependent viruses that one may receive, we also computed the traveling distance L_x for different d_0 and weather conditions (Figure S6 (b)). By combining Figure S6 (a) and (b), we are able to plot the distance-dependent viral load in Figure S7, which characterizes the effectiveness of social distancing at different distances.

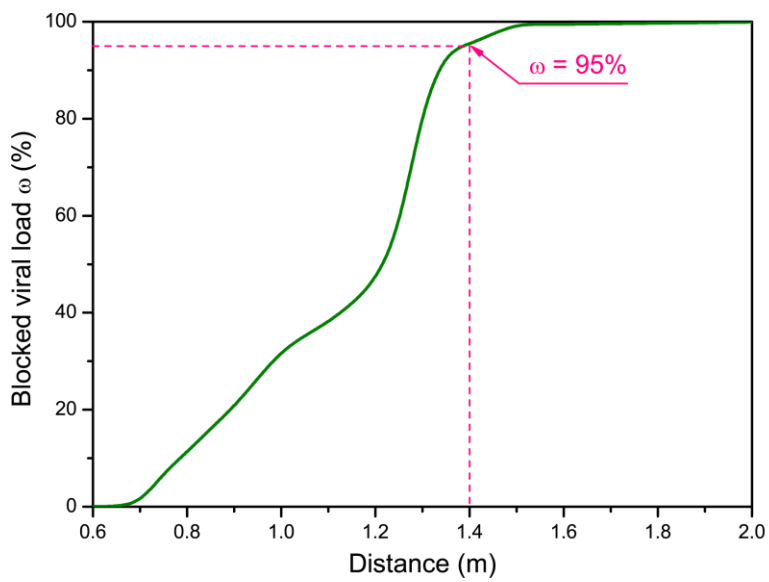

Figure S7. Effectiveness of practicing social distancing at different distance

Figure S6 (b) presents the traveling distance of different droplets at four weather extremes, i.e., cold and humid (T_∞ = 4 °C, RH = 0.88), cold and dry (T_∞ = 4 °C, RH = 0), hot and dry (T_∞ = 36 °C, RH = 0), hot and humid (T_∞ = 36 °C, RH = 0.88). We find that the horizontal traveling of small droplets (d_0 <100 μm) is strongly dependent on weather conditions; however, large droplets are inert and become insensitive to weather change. Since most pathogens exist in large respiratory droplets, the curve of distance-dependent viral load in Figure S7 is not sensitive to weather conditions. Therefore, we only demonstrate the viral load curve under normal indoor conditions (T_∞ = 23 °C, RH = 0.50, V_{air} = 0.3 m/s), and a weather-independent criterion can be used for relaxed social distancing.

Suspension time and total mass of aerosol particles

By integrating equation (S17), the suspension time t_s that is required for a particle to deposit on the ground can be calculated as:

$$v_e t_s + (v_t - v_e)\tau\left(1 - \exp\left(-\frac{t_s}{\tau}\right)\right) = \frac{L_m}{2} - L_z \tag{S19}$$

We then calculated the average suspension time t_m of PM2.5 under different weather conditions, as shown in Figure S8(a). Generally, PM2.5 can suspend in air for around 10 hours. We also find that the hot and dry temperature gives rise to a longer suspension time for PM2.5, as shown in Figure S9(b). The suspension time t_s varies dramatically from 4 hours to around 10 hours when the diameter changes from 10 μm to 1 μm.

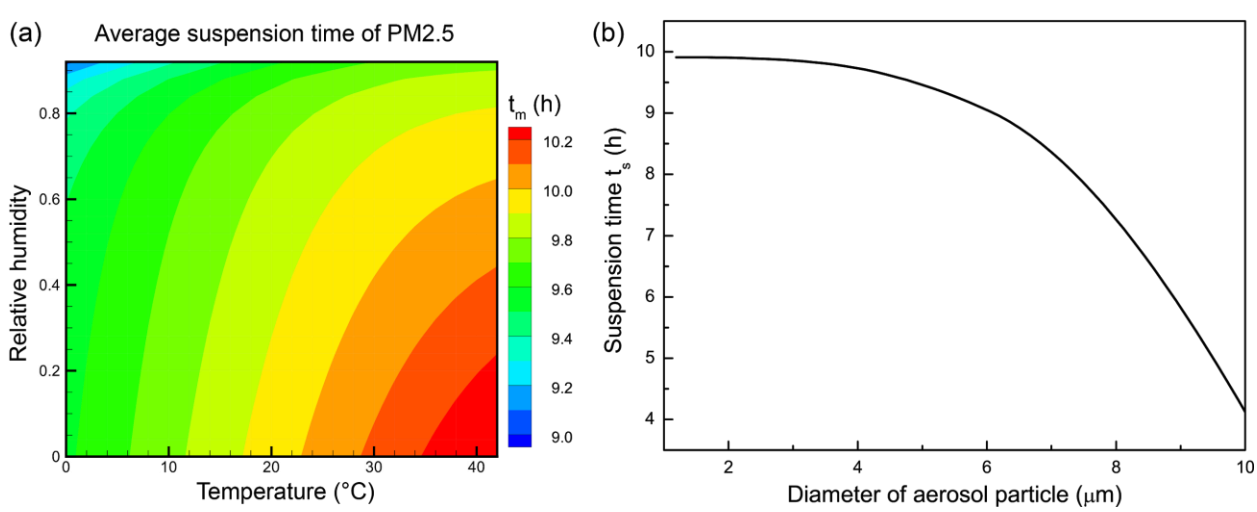

Figure S8. Average suspension time of PM2.5 under different weather conditions

Assume the percentage of droplets that can turn into PM2.5 in speech droplets is $p(d_0)$. d_r is the diameter of the aerosol particle after dehydrating. Then the number of PM2.5 that can be produced by constant speaking is $\sum_{d_0} Np(d_0)$, where N is the number of produced droplets per second. After t_s, the number of the corresponding aerosol particles reaches equilibrium, as the number of newly produced particles is now equal to that of aerosol particles falling on ground. Therefore, the total mass of PM2.5 can be calculated:

$$m_d = \rho_s \sum_{d_r < 2.5} \frac{1}{6} \pi d_r^3 Np(d_0)\, t_s(d_0) \tag{S20}$$

In this study, N is equal to 50 droplets per minute.(*6*) Based on equation S20, the total mass of PM2.5 has been computed under different weather conditions in Figure 3(d).

REFERENCES

1. X. Xie, Y. Li, A. Chwang, P. Ho, W. Seto, How far droplets can move in indoor environments–revisiting the Wells evaporation-falling curve. *Indoor Air*. **17**, 211–225 (2007).
2. J. Kukkonen, T. Vesala, M. Kulmala, The interdependence of evaporation and settling for airborne freely falling droplets. *J. Aerosol Sci.* **20**, 749–763 (1989).
3. M. Kulmala, T. Vesala, Condensation in the continuum regime. *J. Aerosol Sci.* **22**, 337–346 (1991).
4. J. P. Duguid, The size and the duration of air-carriage of respiratory droplets and droplet-nuclei. *Epidemiol. Infect.* **44**, 471–479 (1946).
5. W. E. Ranz, W. R. Marshall, Evaporation from drops. *Chem Eng Prog*. **48**, 141–146 (1952).
6. S. Asadi, A. S. Wexler, C. D. Cappa, S. Barreda, N. M. Bouvier, W. D. Ristenpart, Aerosol emission and superemission during human speech increase with voice loudness. *Sci. Rep.* **9**, 1–10 (2019).